PROCEEDINGS, 43rd Workshop on Geothermal Reservoir Engineering
Stanford University, Stanford, California, February 12-14, 2018
SGP-TR-213

The 2017 Ayvacık Earthquake Sequence: A Listric Fault Activated Beneath Tuzla/Çanakkale Geothermal Reservoir (Western Turkey)

Fatih Bulut[1], Emre Havazlı[2], Cenk Yaltırak[3], Aslı Doğru[1], Aslı Sabuncu[1] and Haluk Özener[1]

[1]Bogazici University, Kandilli Observatory and Earthquake Research Institute, Department of Geodesy, Istanbul, Turkey 34684

[2] University of Miami, Division of Marine Geology and Geophysics, 4600 Rickenbacker Causeway Miami, FL 33149

[3] Istanbul Technical University, Faculty of Mines, Department of Geological Engineering, Ayazaga, Istanbul, Turkey 34426

Contact: bulutf@boun.edu.tr

Keywords: Induced seismicity, 2017 Ayvacık Earthquake, Listric Fault, Western Turkey, Tuzla/Çanakkale Geothermal Reservoir

ABSTRACT

We investigate seismo-geodetic behavior of the Earth's crust during the 2017 Ayvacık earthquake sequence in Western Turkey. The activated fault did not accommodate any M≥5.0 earthquake during instrumental period except the recent sequence of M≥5.0 earthquakes in 2017. High-resolution earthquake locations identified that these earthquakes and associated pre- and aftershocks have activated a listric fault below Tuzla/Çanakkale geothermal reservoir. InSAR images show that the whole process led to a subsidence of ~8 cm in line-of-sight (LOS). The results show that the seismic activity started almost at the surface and systematically propagated downward as well as sideward through the entire listric fault reaching down to the seismogenic basement. Results verify that seismographs are indispensible instruments to identify structural variation as well as to implement hazard mitigation measures in geothermal fields.

1. INTRODUCTION

Changing underground pore-pressure equilibrium activates the faults generating from minor to moderate size earthquakes (Ellsworth, 2013). Monitoring seismic and a-seismic reactions of the Earth's crust against industrial hydraulic processes is therefore of great importance for understanding these human-made earthquakes. In this context, we characterize seismic and a-seismic behavior of a fault beneath a high-enthalpy geothermal reservoir in Tuzla/Çanakkale, in Western Turkey (Karamanderesi, 1986). There, NE-SW oriented extensional regime predominantly governs the seismotectonics (Yaltırak et al, 2012). Recently, the region accommodated four M≥5.0 earthquakes and their intense aftershocks that have sequentially activated a listric fault. In this study, we combined geodetic and seismological data to characterize surface and subsurface movements associated with the 2017 Ayvacık M≥5.0 earthquake sequence. Sentinel-1 InSAR images are used to characterize subsidence and high-resolution earthquake locations are used to identify space-time evolution of the seismic activity along the Tuzla Fault beneath a geothermal reservoir.

2. SEISMOTECTONIC SETTING

The target region is located on one of the trans-tensional extensions of the North Anatolian Fault Zone (NAFZ) into the North Aegean Sea. It is characterized by a NW-SE striking extensional basin merging two NE-SW striking segments of the dextral NAFZ. The rotational wedges links NE–SW striking dextral faults to and NW–SE striking normal faults. There, the North Anatolian Fault Zone reaches to the Aegean Sea near Behramkale extending into the Bababurnu pull-apart basin (Yaltirak et al., 2012). The region was shaken by the 1845, the 1867 and the 1889 earthquakes, respectively (Özden et al., 2018).

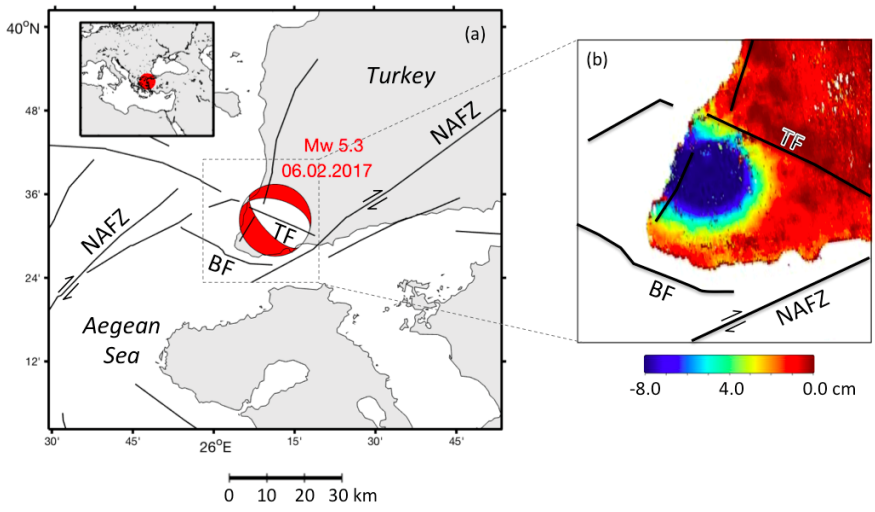

Figure 1: (a) Simplified tectonic map of the target region. Black lines are active faults. NAFZ: North Anatolian Fault Zone, BF: Bababurnu Fault (Yaltırak et al., 2012) and TF: Tuzla Fault (Sözbilir et al., 2017). Beachball shows the focal mechanism of the mainshock. Inset shows the location of target region on regional scale. (b) InSAR-derived subsidence in LOS.

During instrumental period, the region hosted two moderate size earthquakes (1972 M 5.1, 1944 M 5.2). None of them activated Tuzla Fault that has been activated during the 2017 sequence (Sözbilir et al., 2017). This fault is sub-parallel to the northeastern margin of the Bababurnu pull-apart basin. Figure 1 summarizes all these seismotectonics details.

3. RESULTS

We investigated over 5000 seismic events in the vicinity of the 2017 mainshock that have been detected by Kandilli Observatory and Earthquake Research Institute (KOERI hereafter) during the time period of 2016-2018. Activated fault is approximately 15 km long and 15 km deep. Seismic moments of the events are used to estimate event-based average slip and therefore to characterize time history of cumulative slip on the fault. Seismic moments are obtained from earthquake magnitudes (Kanamori, 1983). Following Aki, (1966) average slip is calculated for the 15 x 15 km approximate fault area assuming shear modulus of 32 GPa (Earth's crust), which is then used to investigate history of cumulative slip on the fault for the time period of 2017.01.01 – 2017.04.01.

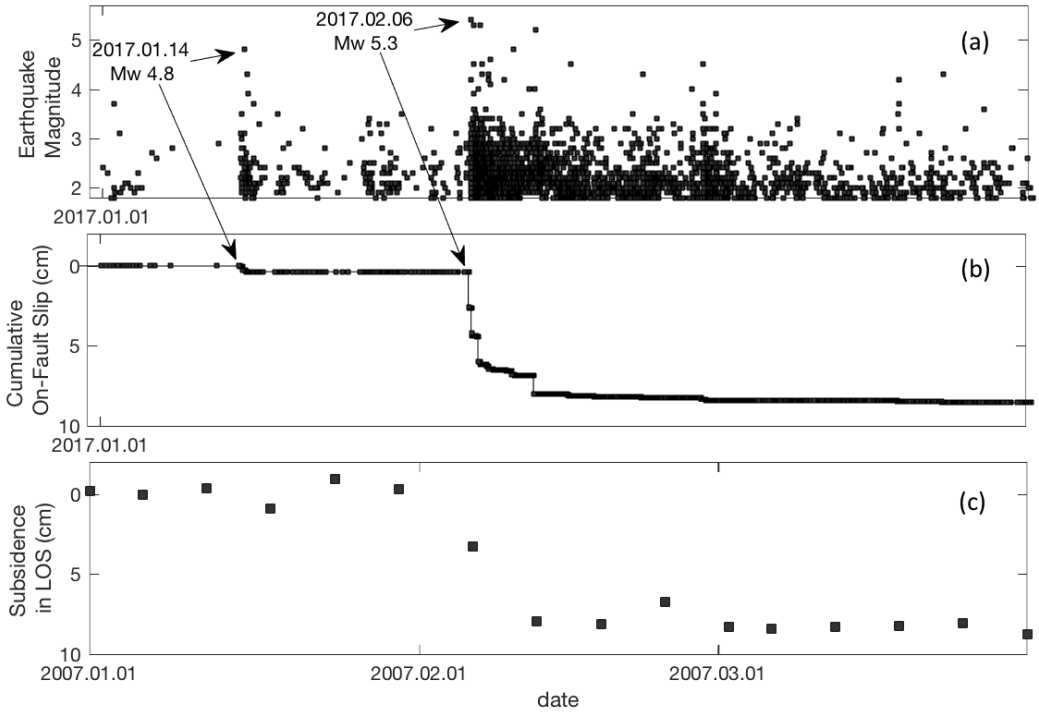

Figure 2: (a) Temporal evolution of the seismicity. (b) Cumulative slip on the activated fault. (c) In LOS (line-of-sight) subsidence in the vicinity of the mainshock. X axes are limited to the same time frame.

Temporal evolution of earthquake magnitudes and associated on-fault slip is shown in Figure 2a and Figure 2b, respectively. There are occasions that fault slips obviously above the background level. These occasions are dominated by four M≥5.0 earthquakes (Figure 2a). We compared seismicity-derived on-fault slip with InSAR-derived subsidence at surface in Figure 2. Seismic data has a temporal resolution of seconds while InSAR data has a temporal resolution of weeks (Geudtner et al., 2012).

Seismicity identifies instant changes of on-fault slip and InSAR detects only its large-scale impulses at surface. The total on-fault slip reaches up to 8 cm (Figure 2b). This is verified by the InSAR derived surface subsidence (Figure 2b). InSAR data shows some sub-centimeter fluctuations. First little fluctuation is detected preceding the 2017.02.06 Mw 5.3 mainshock by seismicity data following the 2017.01.14 Mw 4.8 earthquake (Figure 2b). InSAR confirmed this observation on a lower temporal resolution (Figure 2c). This event was very close to the 2017.02.06 Mw 5.3 mainshock. Therefore, seismographs are indispensible instruments to implement hazard mitigation measures surrounding the geothermal reservoirs. The mainshock initiated a process of totally 8 cm on-fault slip lasting almost three weeks on the Tuzla Fault. Spatial detail of this process is further resolved by high-resolution earthquake locations.

We use the double-difference earthquake location method to obtain the highest earthquake locations (Waldhauser and Ellsworth, 2000). The method utilizes relative arrival time data of closely spaced events to suppress the effect of unmodeled velocity structure on hypocentral offsets, as the ray paths of paired events are almost identical. The method also allows the use of differential travel times, which can be measured much more precisely than arrival time onsets, resulting in more accurate differential locations. Structural characterization is important not only to understand the seismotectonics but also to ensure sustainable use of geothermal reservoirs (Brehme et al., 2016). We used 1D crustal model by Bulut et al., 2009. To achieve the best possible azimuthal coverage, we combined all available seismographs that are operated by KOERI and AFAD.

High-resolution earthquake catalog is subdivided into three time slots to investigate spatiotemporal evolution of the physical process associated with the 06.02.2017 Mw 5.3 earthquake. Selected time slots refer to the preshocks (2017.01.01-2017.02.06), early aftershocks (2017.02.06-2017.03.06) and late aftershocks (2017.03.06-2017.04.06) (Figure 3). The preshocks are localized in the west of the Tuzla Fault (Figure 3a). The hypocentral depths range from 1.0 to 7.0 km. Early aftershocks enlarge the fractured area both horizontally and vertically (Figure 3b). Their hypocentral depths range from 0.0 to 10.0 km. Late aftershocks continue to

enlarge the fractured area both horizontally and vertically activating almost the entire Tuzla Fault (Figure 3c). Majority of the aftershocks remain in the western section of the Tuzla Fault. This is in agreement with the location of InSAR-detected subsidence (Figure 1b). Their hypocentral depths reach down to 14.0 km.

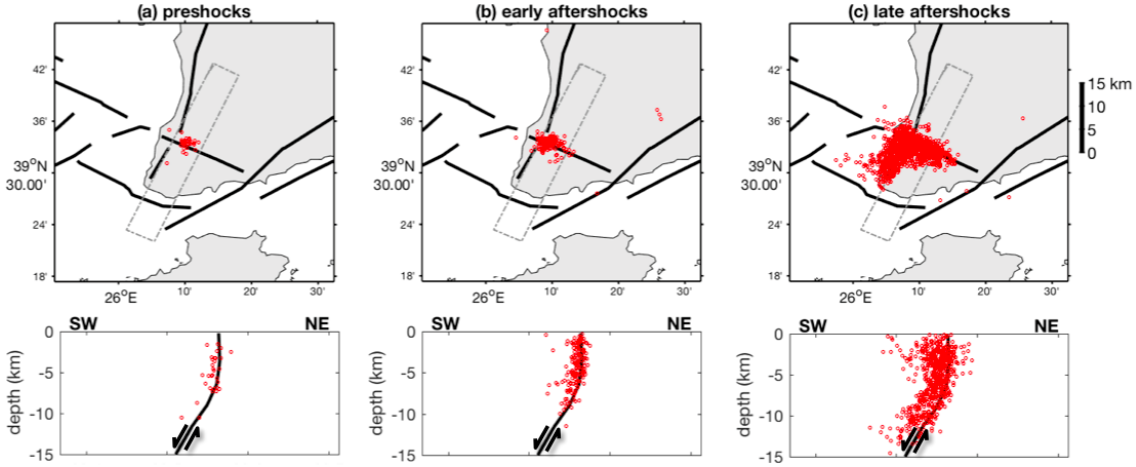

Figure 3: Spatiotemporal evolution of the seismicity associated with the 06.02.2017 Mw 5.3 Earthquake. Upper panel shows map views of faults (black lines), earthquakes (red dots) and location of depth sectional profile (dashed lines). Lower panel shows depth sectional views of Tuzla Fault (black line) and earthquakes (red dots) along a SW-NE profile.

Overall spatiotemporal pattern of the hypocenters shows that the seismic activity started close to the surface and systematically propagated downward as well as sideward activating the entire fault down to the seismogenic basement. High-resolution hypocenters verify the interpretation by Sözbilir et al., 2017 that the Tuzla Fault is a SW-dipping listric fault, of which the inclination becomes systematically shallower with increasing depth. The inclination of the Tuzla Fault changes predominantly around ~7.0 km depth (Figure 3 – lower panel).

4. CONCLUSIONS

(1) The Tuzla Fault accommodated totally ~8 cm slip during the sequence of M≥5.0 earthquakes in 2017. This is verified by the InSAR-derived surface subsidence. (2) A little slip fluctuation (<1 cm) is detected on the fault preceding the 2017.02.06 Mw 5.3 mainshock by seismicity and confirmer by InSAR. (3) The mainshock initiated a fracturing process lasting almost three weeks on the Tuzla Fault. (4) Overall spatiotemporal pattern of the hypocenters shows that the seismic activity started close to the surface and systematically propagated downward as well as sideward activating the entire fault down to the seismogenic basement. (5) High-resolution hypocenters verify that the Tuzla Fault is a SW-dipping listric fault, where the inclination becomes systematically shallower with increasing depth. The inclination changes predominantly around ~7.0 km depth. (6) To sum up, seismographs are indispensible instruments to identify structural variation as well as to implement hazard mitigation measures in geothermal fields.

REFERENCES

Aki, K. (1966). Generation and Propagation of G Waves from the Niigata Earthquake of June 16, 1964: Part 1. A statistical analysis.

Bulut, F., Bohnhoff, M., Ellsworth, W. L., Aktar, M., & Dresen, G. (2009). Microseismicity at the North Anatolian fault in the Sea of Marmara offshore Istanbul, NW Turkey. *Journal of Geophysical Research: Solid Earth*, *114*(B9).

Brehme, M., Blöcher, G., Cacace, M., Kamah, Y., Sauter, M., & Zimmermann, G. (2016). Permeability distribution in the Lahendong geothermal field: A blind fault captured by thermal–hydraulic simulation. *Environmental Earth Sciences*, *75*(14), 1088.

Ellsworth, W. L. (2013). Injection-induced earthquakes. *Science*, *341* (6142), 1225942.

Geudtner, D.; Torres, R.; Snoeij, P.; Davidson, M. (2012), Sentinel-1 System Overview. In Proceedings of the 9th European Conference on Synthetic Aperture Radar, Nürnberg, Germany, 23–26 April 2012; pp. 159–161.

Kanamori, H. (1983). Magnitude scale and quantification of earthquakes. Tectonophysics, 93 (3-4), 185-199.

Karamanderesi, I. H. (1986). *Hydrothermal alternation in well Tuzla T-2, Canakkale, Turkey* (No. 3). United Nations University.

Özden, S., Över, S., Poyraz, S. A., Güneş, Y., & Pınar, A. (2018). Tectonic implications of the 2017 Ayvacık (Çanakkale) earthquakes, Biga Peninsula, NW Turkey. *Journal of Asian Earth Sciences*, *154*, 125-141.

Sözbilir, H., Uzel, B., Sümer, Ö., Eski, S., Softa, M., Tepe, Ç., Ozkaymak, C. and Baba, A. (2017). Çanakkale-Ayvacık Deprem Fırtınasının (14 Ocak-20 Mart 2017) Sismik Kaynakları, *4rd International Conference on Earthquake Engineering and Seismology (4ICEES) Oct 11-13 2017 – Anadolu University – Eskisehir/Turkey (In Turkish).*

Waldhauser, F., & Ellsworth, W. L. (2000). A double-difference earthquake location algorithm: Method and application to the northern Hayward fault, California. *Bulletin of the Seismological Society of America*, *90*(6), 1353-1368.

Yaltırak, C., İşler, E. B., Aksu, A. E., & Hiscott, R. N. (2012). Evolution of the Bababurnu Basin and shelf of the Biga Peninsula: western extension of the middle strand of the North Anatolian Fault Zone, Northeast Aegean Sea, Turkey. *Journal of Asian Earth Sciences*, *57*, 103-119.